

The bulge region of HIV-1 TAR RNA binds metal ions in solution

Mikołaj Olejniczak, Zofia Gdaniec*, Artur Fischer, Tomasz Grabarkiewicz, Łukasz Bielecki and Ryszard W. Adamiak

Institute of Bioorganic Chemistry, Polish Academy of Sciences, Noskowskiego 12/14, 61-704 Poznań, Poland

Received May 21, 2002; Revised and Accepted August 6, 2002

ABSTRACT

Binding of Mg²⁺, Ca²⁺ and Co(NH₃)₆³⁺ ions to the HIV-1 TAR RNA in solution was analysed by ¹⁹F NMR spectroscopy, metal ion-induced RNA cleavages and Brownian dynamics (BD) simulations. Chemically synthesised 29mer oligoribonucleotides of the TAR sequence labelled with 5-fluorouridine (FU) were used for ¹⁹F NMR-monitored metal ion titration. The chemical shift changes of fluorine resonances FU-23, FU-25 and FU-40 upon titration with Mg²⁺ and Ca²⁺ ions indicated specific, although weak, binding at the bulge region with the dissociation constants (*K_d*) of 0.9 ± 0.6 and 2.7 ± 1.7 mM, respectively. Argininamide, inducing largest ¹⁹F chemical shifts changes at FU-23, was used as a reference ligand (*K_d* = 0.3 ± 0.1 mM). In the Pb²⁺-induced TAR RNA cleavage experiment, strong and selective cleavage of the C24-U25 phosphodiester bond was observed, while Mg²⁺ and Ca²⁺ induced cuts at all 3-nt residues of the bulge. The inhibition of Pb²⁺-specific TAR cleavage by di- and trivalent metal ions revealed a binding specificity [in the order Co(NH₃)₆³⁺ > Mg²⁺ > Ca²⁺] at the bulge site. A BD simulation search of potential magnesium ion sites within the NMR structure of HIV-1 TAR RNA was conducted on a set of 20 conformers (PDB code 1ANR). For most cases, the bulge region was targeted by magnesium cations.

INTRODUCTION

RNA in its diverse structural forms plays a key role in many biological processes. Its polyanionic structure is highly dependent on the presence of monovalent and divalent metal ions (1,2). Although the vast majority of cations bind RNA non-specifically, a subset of metal ions interacts more or less strongly with specific sites (3–5). High resolution X-ray crystallography, capable of determining hydration spheres of cations, is the principal method that allows for accurately locating and characterising RNA/metal ion binding sites. Our knowledge on RNA ion binding sites is still based on

relatively few X-ray structures, among them tRNAs (6,7), hammerhead ribozyme (8), group I intron (9), leadzyme (10) and RNA duplexes (11). As elevated salt concentration is often required for the growth of an RNA crystal, a definite characterisation of specific ion-binding sites of functional importance might be accomplished only when combining results of structure analysis both in crystal and in solution. Conventional techniques of ¹H NMR spectroscopy usually do not give direct information on RNA ion binding sites. Therefore, use of the Co(NH₃)₆³⁺ ion mimicking Mg(H₂O)₆²⁺ has been offered (12,13) to solve the NMR structure of RNA/metal binding sites with a high resolution.

The ¹⁹F NMR spectroscopy offers an attractive alternative to study RNA/metal binding (14,15). ¹⁹F chemical shifts are extremely sensitive to an altered local environment of a nucleus, thus making fluorine an ideal NMR spin label for the study of nucleic acids interactions. Other advantages of using fluorine are the high intrinsic NMR sensitivity of the ¹⁹F nucleus (83% of the proton sensitivity) and 100% natural abundance. It has been shown that in spite of lower p*K_a* of 5-fluorouridine (FU) (in comparison with uridine), FU substitution has only a negligible influence on the NMR structure of RNA duplexes (14,16,17). The ¹⁹F NMR spectroscopy was used previously to study conformational heterogeneity in RNA under various solution conditions (18,19). While our work was in progress, ¹⁹F NMR spectroscopy was applied for the analysis of metal ion-induced folding of the hammerhead ribozyme (20).

Biochemical methods of probing metal ion binding to RNA (2) include ion-induced specific cleavage of RNA, various competitive inhibition experiments and phosphorothioate interference assays. The method based on metal ion-induced RNA cleavage has already been proposed for the identification of metal ion-binding sites in tRNA (21), 16S and 23S rRNA (22), HDV ribozyme (23), RNase P RNA (24) and group I intron (25). In its competitive inhibition version (26), the method takes advantage of the competition between different metal ions that bind to a common specific site and are mutually exclusive. In addition, this approach provides information concerning the relative affinities of metal ions to this specific site. This method was successfully used in the localisation of metal ion binding sites in the group I intron (27), 16S and 23S rRNA molecules (28).

*To whom correspondence should be addressed. Tel: +48 61 8528503; Fax: +48 61 8520532; Email: zgdan@ibch.poznan.pl

Recently, modelling of RNA/metal binding sites by computer simulation with the use of molecular mechanics based on a docking principle (29,30) and Brownian dynamics (BD) (31) were proposed. In the BD simulation positively charged test spheres, which mimic cations under study, diffuse under the influence of random motion in the electrostatic field of the rigid RNA molecule. The BD simulation allowed for a good reproduction of X-ray determined RNA/metal sites and NMR determined RNA/Co(NH₃)₆³⁺ sites (31). It was also offered as an interesting prediction tool in the case of NMR solution structures in which metal ions were not localized (31–33).

The TAR RNA element is located at the 5'-end of all HIV-1 mRNAs and its interactions with the *trans*-activator (Tat) protein and several cellular proteins play a crucial role in the *trans*-activation of viral transcription (34). The importance of these interactions makes TAR RNA a target for therapeutic strategies (35). The structure of the HIV-1 TAR RNA as a ligand-free molecule (36) or in a complex with argininamide (37–39), Tat-derived peptides (37,40) or neomycin (41) was investigated by NMR (36,39,40) and molecular dynamics studies (38,42). It was found (36) that in solution, bulged residues U23 and C24 of ligand-free TAR RNA are stacked within the helix and U25 is looped out. The stacked structure of the bulge induces a bending of the overall helix axis (43).

There are very limited data available on HIV-1 TAR RNA interactions with metal ions. Until now, no X-ray structure of the HIV-1 TAR RNA hairpin has been reported. However, the structure of RNA duplex comprising the bulge region of TAR RNA but devoid of the apical loop was solved at 1.3 Å resolution (44). In crystal, the conformation of the bulged backbone is stabilised by three calcium ions, one of which directly interacts with three phosphate groups (U23, C24 and G26). An additional calcium ion was found in the major groove of the TAR fragment. The authors suggested that the presence of calcium ions in the crystal structure might be indicative of a potential divalent metal ion-binding site within the native TAR RNA. However, due to the high concentration of CaCl₂ required for crystallization (100 mM), far from physiological conditions, one might question the importance of divalent metal ions in TAR RNA stabilisation.

Does the HIV-1 TAR RNA hairpin bind magnesium or other divalent metal cations in solution? So far, there has been no direct structural evidence available. It should be underlined that magnesium was absent from the conditions of all NMR studies of HIV-1 TAR RNA already published (36,37,39–41). One observation with regard to the TAR RNA interaction with metal ions in solution comes from transient electric birefringence studies (45). In that experiment, a 120-nt long RNA duplex containing the bulge region of TAR RNA was analysed. It was noted that 2 mM Mg²⁺ induced a partial straightening of the RNA molecule studied, which is otherwise bent at the bulge region. Another observation concerns destabilisation of the HIV-1 TAR/Tat-peptide complex by Mg²⁺ ions (46). The fluorescence intensity of the complexes formed between the TAR RNA hairpin, labelled with a fluorescent base at position 24 of the bulge, and Tat-derived peptides was quenched upon the addition of Mg²⁺ and reached the free TAR RNA level at a 10 mM Mg²⁺ concentration.

Here, we would like to report the results of ¹⁹F NMR-monitored titrations, metal ion-specific cleavages and the competitive inhibition of Pb²⁺-induced cleavage which clearly

indicate that Mg²⁺, Ca²⁺ and Co(NH₃)₆³⁺ ions bind specifically, although weakly, within the bulge region of the TAR RNA hairpin. Argininamide, used as a reference ligand during ¹⁹F NMR experiments, binds to the TAR RNA bulge in a single binding mode. It also competes with Pb²⁺ for the same binding site. To complement experimental results, BD simulations were accomplished on a set of 20 TAR conformers. The collected data revealed that for 14 out of 20 RNA cases the region composed of the bulge and flanking base pairs of both stems was targeted by magnesium cations. We believe that the results presented will increase the interest in combining experimental and computational approaches for the exploration of moderately weak metal ion RNA binding sites in solution.

MATERIALS AND METHODS

Materials and oligoribonucleotide synthesis

T4 polynucleotide kinase was purchased from MBI Fermentas. RNase T1 was obtained from Boehringer. [³²P]ATP (5000 Ci/mmol) was purchased from ICN. Other materials used in this study were either from Sigma or Aldrich.

The synthesis of 29mers of HIV-1 TAR RNA, both unmodified and modified with FU, was performed using solid-support aided phosphoramidite chemistry and applying the 2'-*O*-tBDMSi protection (47). After 1 μmol scale synthesis and deprotection with fluoride anion, the oligoribonucleotides were purified by preparative 19% polyacrylamide gel electrophoresis (PAGE) in denaturing conditions, followed by electroelution with Biotrap BT 1000 (Schleicher & Schuell) and desalting on NAP columns. The RNAs were isolated with average 10% total yields of synthesis and purification. Primary structure of oligoribonucleotides was confirmed by sequencing with ribonuclease T1 (G-specific RNase) and MALDI-TOF spectrometry.

¹⁹F NMR spectroscopy

NMR data were acquired on a Varian Unity 300 spectrometer equipped with selective ¹⁹F/¹H probe (5 mm). The ¹⁹F base frequency was 282.19 MHz. Data were accumulated with a relaxation delay of 1 s over a spectral width of 11 611 Hz by using 16 K points. A total of 1000–4000 scans were averaged to achieve good signal to noise ratio. Prior to the Fourier transformation, exponential line broadening 4–8 Hz was applied to FIDs. Fluorine chemical shifts were referenced to external FU.

RNA concentrations ranged from 0.1 to 0.2 mM and were determined from the absorbance at 260 nm. Stock solutions of MgCl₂, CaCl₂, Co(NH₃)₆Cl₃ or argininamide dihydrochloride were prepared. Aliquots of the solutions were added directly to the RNA sample in an NMR tube. The buffer used was 10 mM sodium phosphate, 50 mM NaCl, 0.1 mM EDTA (pH 6.6). In the Ca²⁺ titration experiment, to provide buffer conditions comparable with those used in the X-ray study (44), 10 mM sodium cacodylate pH 6.5, 50 mM NaCl and 0.1 mM EDTA were used. The binding of ligands to FU-TAR RNAs was measured quantitatively using ¹⁹F NMR spectroscopy. Binding curves were obtained by monitoring fluorine chemical shifts changes upon titration of the RNA with ligand solutions at the constant temperature of 21 ± 0.5°C. The

equilibrium dissociation constants (K_d) were estimated by non-linear curve fitting based on the previously published equation for RNA/ligand in a fast exchange (41,48,49). The only satisfactory fit was obtained using 1:1 stoichiometry for all ligands studied. The average dissociation constants were estimated only for fluorine resonances with a significant chemical shift dependence on metal ion concentration.

Metal ion-induced RNA phosphodiester bond cleavages

The oligoribonucleotides were 5'-end labelled using T4 polynucleotide kinase and [γ - 32 P]ATP according to standard procedures. Subsequently, they were purified by denaturing 19% PAGE, eluted from the gel by crush-and-soak method, precipitated with ethanol, redissolved in sterile water, and quantified by a Beckman LS5000TA scintillation counter. Prior to the analysis, the RNA hairpins (~30 000 c.p.m.) were refolded by heating at 90°C for 30 s followed by slow cooling to the room temperature. For Pb $^{2+}$ ion-induced cleavage reaction, refolding was performed in a buffer containing 10 mM Tris-HCl pH 7.2, 40 mM NaCl and 8 μ M carrier tRNA. Afterwards, freshly prepared Pb(OAc) $_2$ solution was added to the final concentrations of 0.5, 1 and 2 mM. The 10 μ l reaction mixture was incubated for 15 min at the room temperature. For Mg $^{2+}$ or Ca $^{2+}$ ion-induced cleavage reactions, refolding was performed in a solution containing 40 mM NaCl, 8 μ M carrier tRNA and 0.025 mM EDTA. Immediately afterwards, the buffer solution was added to a final concentration of 10 mM Tris-HCl pH 8.5. Subsequently, either MgCl $_2$ or CaCl $_2$ solution was added to the final concentrations of 0.5, 1 and 2 mM. The 10 μ l reaction mixture was incubated for 15 h at 37°C. All reactions were quenched by the addition of an equal volume of gel loading buffer (8 M urea, 20 mM EDTA, tracking dyes) and stored on dry ice. Reaction products were separated by 19% PAGE (8 M urea). The results were visualised and quantitatively analysed using phosphorimaging screens and a Typhoon 8600 Imager with ImageQuant software (Molecular Dynamics). The images were not edited and a linear relationship between signal and image intensity was retained.

Inhibition of Pb $^{2+}$ -induced cleavage

For competitive inhibition of Pb $^{2+}$ -induced RNA cleavage, the oligoribonucleotides were 5'-end labelled and refolded as described above for the Pb $^{2+}$ cleavage reaction. The cleavage with Pb $^{2+}$ ions was performed at a constant 2 mM concentration of Pb $^{2+}$ ions and in the presence of increasing concentrations of MgCl $_2$, CaCl $_2$, Co(NH $_3$) $_6$ Cl $_3$ or argininamide dihydrochloride, at the room temperature for 15 min. The concentrations of competing metal ions and argininamide are specified in the legend to Figure 4. The reaction products were quantitatively analysed as described above. The concentration of competing ions necessary for the 50% inhibition of cleavage (IC $_{50}$) was calculated from the plot of the relative intensity of Pb $^{2+}$ -induced cleavage at C24 versus the concentration of competing ions.

Brownian dynamics simulations

Atomic coordinates of a ligand-free HIV-1 TAR RNA structure were taken from the Brookhaven Protein Data Bank (PDB code 1ANR). The whole set of 20 conformers satisfying NMR constraints (36) was subjected to the analysis.

These conformers are identified here by numbers 1–20, which correspond to their order in the PDB file. The UHBD program (50) was used to simulate a random motion of metal ions within the electrostatic field of the RNA molecule. Parameters concerning electrostatics and details of the BD simulation followed those from the original report (31). The diffusing Mg(H $_2$ O) $_6^{2+}$ cations were modelled as positively charged spheres of optimised radii 2.2 Å and +2e charge. Trajectories of test spheres were started at randomly chosen points at a distance of 100 Å from the centre of mass of the rigid TAR molecule. Test spheres that stayed within the cut-off sphere of radius 180 Å were simulated for 200 ns at a time step of 0.02 ps. For each test sphere, 1000 trajectories were calculated. Calculations were carried out on a SGI Origin 3200 platform.

All recorded probe coordinates (10 6) were taken into account. Geometries of potential binding sites were visualised using the InsightII/Delphi software package (Accelrys). For this purpose, all trajectory data from UHBD were converted into the InsightII format. As a result, a file containing 'numbers of contacts' was obtained. The 'number of contacts' is defined as a sum of single events when the modelled cation sphere was recorded at the certain point in space, during the trajectory. Obtaining that, it was possible to create three-dimensional contours that comprised points of the same values, reflecting the probability of magnesium ions location. To perform structural analysis, these contours (shown in yellow; see Fig. 5) were superimposed on the rigid RNA structures using a cubic grid of 1 Å spacing. This allowed for indication of TAR residues and atoms of close proximity (4 Å) to potential magnesium location, for all 20 conformers. For evaluation of site-occupancy statistics, the resulting data were categorised into three groups, according to the numbers of contacts: high (>2.5 · 10 4); medium (10 4 –2.5 · 10 4) and low (<10 4).

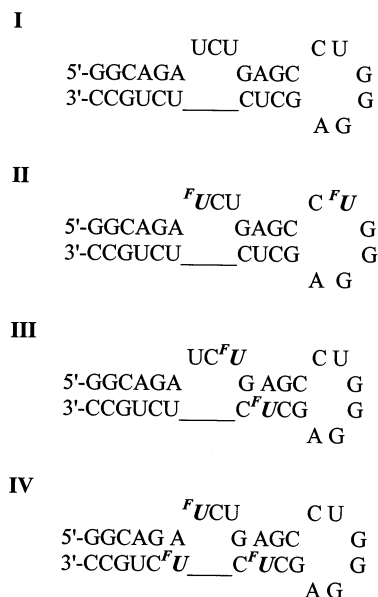
A reference experiment, conducted for testing the above protocol at the initial stage of our study, fully reproduced the results of BD simulation (31) of the structure of a RNA hairpin/metal binding site (12) (data not shown).

RESULTS AND DISCUSSION

19 F NMR-monitored metal ion titration

For the purpose of this study, a 29mer oligoribonucleotide of HIV-1 TAR RNA sequence (I) and its three regioselectively FU-labelled analogues (II–IV) were chemically synthesised. FU labels were introduced at positions 23, 31 (II), 25, 38 (III) and 23, 38, 40 (IV) as shown in Scheme 1.

Prior to 19 F NMR titration studies, the Pb $^{2+}$ cleavage reaction, discussed below in detail, was carried out to detect potential conformational differences between unlabelled (I) and FU-substituted TAR RNAs (II–IV). The lead-induced cleavage patterns of both unmodified and FU-labelled hairpins were virtually the same using quantitative measures. These results, together with data from previous NMR studies concerning the incorporation of FU into RNA duplexes containing FU-A and FU-G base pairs (16,51), suggested that in our case the incorporation of FU might have only a minor, if any, effect on the 29mer TAR RNA structure. This



Scheme 1.

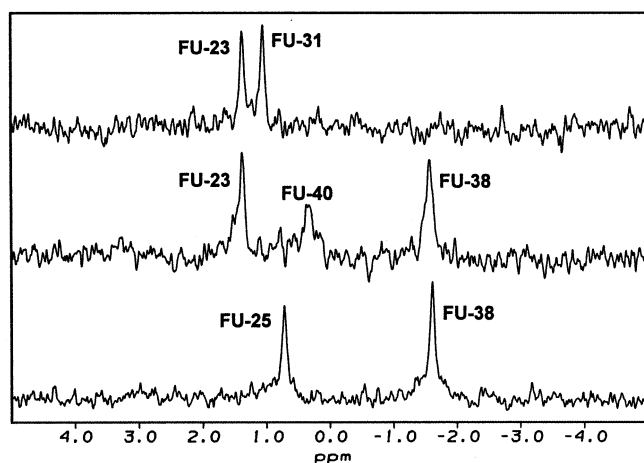


Figure 1. ^{19}F NMR spectra of FU labelled HIV-1 TAR RNA hairpins (II–IV).

allowed us to deal with the FU label as a non-invasive probe in this ^{19}F NMR study.

The unambiguous assignment of well resolved fluorine resonances was accomplished by a comparison of fluorine chemical shifts in ^{19}F NMR spectra of all three FU-modified hairpins as shown in Figure 1. Within molecules II–IV, ^{19}F chemical shifts were assigned as follows: FU-23 (1.57 p.p.m.), FU-25 (0.71 p.p.m.), FU-31 (1.25 p.p.m.), FU-38 (–1.37 p.p.m.) and FU-40 (0.58 p.p.m.). The signal of FU-38 residue, which is located in the upper helical stem, was 1.95–2.94 p.p.m. up-field of unpaired fluorouridine residues, which agrees well with the data for FU-labelled tRNA (15) and RNA hairpin (19) analyses. Significant low-field shift of FU-40 with reference to FU-38 ($\Delta\delta = 1.85$ p.p.m.) probably reflects large perturbation of stacking interactions of base pairs flanking the bulge.

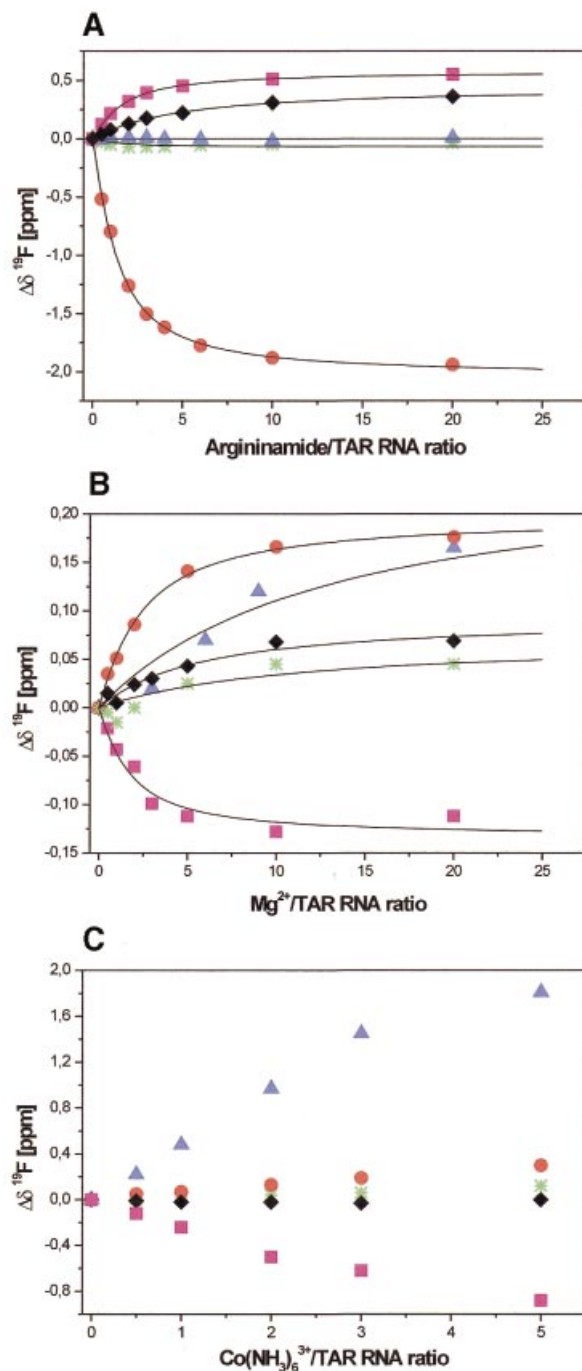


Figure 2. ^{19}F NMR titration of TAR RNA hairpins (II–IV) with argininamide (A), Mg^{2+} (B) and $\text{Co}(\text{NH}_3)_6^{3+}$ (C). Normalised chemical shift changes of FU-23 (red circles), FU-25 (magenta squares), FU-31 (green stars), FU-38 (black diamonds) and FU-40 (blue triangles) are presented. Experimental data for (A) and (B) are shown together with the best fits of a single site binding model.

To test the sensitivity of the ^{19}F chemical shifts of (II–IV) on ligand binding and the extent of information that could be obtained from ^{19}F NMR titration experiments, an appropriate reference ligand should be applied. Therefore, argininamide, which is known to bind specifically to the bulge region of TAR (39), was used. The δ (^{19}F) chemical shift changes versus increasing argininamide/RNA ratio are shown in Figure 2A.

Large chemical shift changes were induced by less than 1 equivalent of argininamide. In the presence of 20 molar excess of argininamide, the resonance of the residue FU-23 ($\Delta\delta = -1.94$ p.p.m.) was the most affected. Only negligible chemical shift changes for FU-31, located in the apical loop, were detected. The resonances of the residues FU-25 and FU-38 were shifted by 0.55 and 0.36 p.p.m., respectively. In the absence of ligand, the FU-40 signal of hairpin IV was much broader than other fluorine resonances. FU-40 resonance sharpened significantly with the addition of argininamide and at the 6-molar excess of ligand its linewidth (29 Hz) was comparable with the others.

^{19}F NMR spectroscopy with the use of our reference ligand allowed for the discussion of the mode of argininamide binding to TAR RNA. The resonance of the FU-23 residue, which is crucial in argininamide binding, was the most affected. The significant shift of the resonances of residues FU-25 and FU-38 upon addition of argininamide is consistent with the previously observed conformational rearrangement within the bulge, which might give rise to a base triple formation between U23 and the base pair A27-U38 (39). The sharpening of FU-40 resonance upon addition of argininamide is in agreement both with the observation on the high solvent exchange found for the U40 imino proton in the flexible ligand-free TAR structure (36) and with the known stabilising effect of argininamide or peptide binding on the lower stem closing the A22-U40 base pair (37). It should be underlined that with the increased argininamide/TAR stoichiometry, only one set of resonances was observed, which is indicative of a complex formation in a fast exchange. Chemical shift profiles as a function of ligand concentration (Fig. 2A) indicated that argininamide binding was specific and saturable. The equilibrium dissociation constant, $K_d = 0.3 \pm 0.1$ mM, was estimated from the analysis of the titration curves. The only satisfactory fit was obtained assuming binding stoichiometry of 1:1. Our results indicate approximately 10 times stronger binding of argininamide to TAR than was calculated before (~2–3 mM) from ^1H chemical shift profiles for A22 (H2) and G28 (H8) of HIV-1 TAR RNA as a function of ligand concentration (39).

The results of ^{19}F NMR analysis of argininamide binding to TAR prompted us to employ this technique to the analysis of Mg^{2+} , Ca^{2+} and $\text{Co}(\text{NH}_3)_6^{3+}$ ions binding to TAR RNA (II–IV). The largest Mg^{2+} -induced chemical shift changes were observed (Fig. 2B) in the region of the bulge for residues FU-23 ($\Delta\delta = 0.18$ p.p.m.), FU-25 ($\Delta\delta = -0.11$ p.p.m.) and for FU-40 ($\Delta\delta = 0.17$ p.p.m.). The addition of Ca^{2+} to II–IV resulted in opposite shifts of fluorine resonance FU-23 ($\Delta\delta = -0.17$ p.p.m.) and larger, up-field shift of FU-40 ($\Delta\delta = -0.40$ p.p.m.) while the residue FU-25 ($\Delta\delta = -0.02$ p.p.m.) was only slightly affected (data not shown). Upon titration with Mg^{2+} or Ca^{2+} ions, the largest $\Delta\text{p.p.m.}$ values of ^{19}F resonances were observed for the residues that are located in the region of the bulge. Only negligible ^{19}F chemical shift changes were observed for the resonance of FU-31 located in the apical loop. These results strongly suggest that there is a metal ion-binding site in the bulge region of HIV-1 TAR RNA.

The K_d values of 0.9 ± 0.6 and 2.7 ± 1.7 mM for Mg^{2+} and Ca^{2+} binding, respectively, correspond to relatively weak binding (13) and they are of the same order as argininamide binding. Moreover, the binding of magnesium ions, which is

necessary for stability or catalytic activity of RNA, is often characterised by K_d values of this order (4,52). Besides, the concentration of magnesium ions in mammalian cells is widely believed to be in the millimolar range with estimations ranging from as little as 1 mM (53) to as much as 30 mM (2).

There is an increasing amount of data to demonstrate that $\text{Co}(\text{NH}_3)_6^{3+}$ can serve as a probe for identification of $\text{Mg}(\text{H}_2\text{O})_6^{2+}$ binding sites in RNA (12,13,30). The ionic radius of $\text{Co}(\text{NH}_3)_6^{3+}$ is similar to that of a hexahydrated Mg^{2+} ion (54). The advantage of using $\text{Co}(\text{NH}_3)_6^{3+}$ for ^1H NMR study, in contrast to $\text{Mg}(\text{H}_2\text{O})_6^{2+}$, is that the exchange-inert property of cobalt complex ions prevents inner-sphere interactions with functional groups of RNA (13). The influence of $\text{Co}(\text{NH}_3)_6^{3+}$ ions on ^{19}F chemical shifts of TAR RNA hairpins II–IV was measured (Fig. 2C). Upon the gradual addition of $\text{Co}(\text{NH}_3)_6^{3+}$, up to 5 molar equivalents, the largest chemical shift changes appeared at FU-23 ($\Delta\delta = 0.27$ p.p.m.), FU-25 ($\Delta\delta = -0.88$ p.p.m.), FU-38 ($\Delta\delta = -0.12$ p.p.m.) and FU-40 ($\Delta\delta = 1.81$ p.p.m.). The chemical shift changes induced by binding of $\text{Co}(\text{NH}_3)_6^{3+}$ are larger than those induced by Mg^{2+} and indicate that $\text{Co}(\text{NH}_3)_6^{3+}$ binds to the bulge region of HIV-1 TAR RNA, although the coordination details may be not the same for the two ions. If more than five equivalents of $\text{Co}(\text{NH}_3)_6^{3+}$ ions were added, the RNA samples irreversibly aggregated. This confirms earlier reports on $\text{Co}(\text{NH}_3)_6^{3+}$ -induced RNA condensation (55). Therefore, we were not able to estimate an equilibrium dissociation constant for the $\text{Co}(\text{NH}_3)_6^{3+}$ complex (56) due to the lack of titration data for $\text{Co}(\text{NH}_3)_6^{3+}$ /TAR RNA ratio higher than five equivalents.

Metal ion-induced HIV-1 TAR RNA cleavages

To obtain a further insight into the binding of metal ions to TAR RNA we employed two approaches, namely, metal ion-induced cleavages of phosphodiester bonds and competitive inhibition experiments. Unmodified hairpin I was used for these studies. In the absence of metal ions, the oligoribonucleotide I was stable at pH 7.2 (57). At pH 8.5, small evenly distributed degradations were observed after 15 h (58).

Ion-induced cleavages of unmodified TAR RNA (I) with Pb^{2+} , Mg^{2+} and Ca^{2+} ions were performed and quantitatively analysed. The cleavage with lead ions was conducted at physiological pH of 7.2 for 15 min and at the room temperature. The incubation with only 0.5 mM Pb^{2+} was sufficient to produce very strong, specific cleavage of TAR RNA at position C24 and secondary, much weaker, cuts at positions A22, U23 and U25 located in the bulge region (Fig. 3). The same pattern was observed for FU modified TAR RNAs (II–IV). The high efficiency of cleavage reaction at position C24 suggests that it was induced by a tightly bound Pb^{2+} ion.

The experimental conditions used for cleavage reaction with Mg^{2+} and Ca^{2+} (pH 8.5, 15 h, 37°C) were quite different from those used for Pb^{2+} catalysed cleavage because of much higher $\text{p}K_a$ values of corresponding metal ion hydrates (21). The patterns and efficiencies of TAR RNA cleavage obtained with Mg^{2+} and Ca^{2+} were very similar to each other (Fig. 3). However, in contrast to Pb^{2+} -induced cleavages, only weak cuts were obtained at 0.5 mM concentration of these ions. In experiments with Mg^{2+} and Ca^{2+} , the intensity of cleavage at C24 was slightly higher than that at U23 and U25 while the cleavage at A22 was the least efficient. Although major

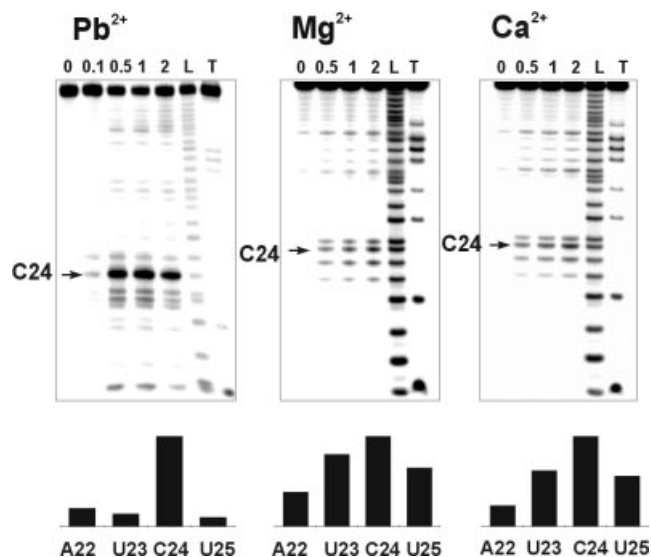


Figure 3. The cleavage reactions of TAR RNA with Pb^{2+} (pH 7.2, 15 min, 37°C), Mg^{2+} (pH 8.5, 15 h, 37°C) and Ca^{2+} (pH 8.5, 15 h, 37°C) ions. The concentrations of cations (mM) are indicated above the lanes. L and T indicate formamide ladder and partial hydrolysis by RNase T1, respectively. The relative intensities of cleavages induced at the bulge region by 0.5 mM Pb^{2+} , 2 mM Mg^{2+} and 2 mM Ca^{2+} are shown below.

cleavages induced by Mg^{2+} and Ca^{2+} ions were located in the bulge region of TAR RNA, smaller cleavages at U31 and A35 of the hexanucleotide apical loop were also observed.

High-resolution NMR studies of the free TAR structure revealed that the bulge region presents some conformational flexibility at U25, and to a lesser extent, at A22, U23 and C24 (36). The dynamic behaviour of HIV-1 TAR was also confirmed by molecular dynamics simulations (38) and NMR residual dipolar couplings that were published very recently (43). In the light of these results, it seems that the cleavage pattern produced by Ca^{2+} and Mg^{2+} ions binding to TAR RNA is likely to be a consequence of flexibility in the bulge region of free TAR and may reflect multiple binding modes of cations to the same site.

Competitive inhibition of Pb^{2+} -specific cleavage by Mg^{2+} , Ca^{2+} , $\text{Co}(\text{NH}_3)_6^{3+}$ and argininamide

In order to explore further the specificity of metal ion binding to the bulge site of TAR RNA, the influence of Mg^{2+} , Ca^{2+} and $\text{Co}(\text{NH}_3)_6^{3+}$ ions on the efficiency of strong and selective Pb^{2+} -induced cleavage at C24 was examined (Fig. 4). The cleavage was effectively inhibited by the increasing concentrations of all these ions, which indicated that competing ions replaced Pb^{2+} from a general metal ion-binding site. In order to extract quantitative information from competitive inhibition experiments, we determined the concentration of competing ions necessary for the 50% inhibition of cleavage (IC_{50}). The obtained values of IC_{50} : 1.6, 7.0 and 9.8 mM for $\text{Co}(\text{NH}_3)_6^{3+}$, Mg^{2+} and Ca^{2+} , respectively, correspond well to the ^{19}F NMR titration data. The quantitative evaluation of competitive inhibition data revealed that $\text{Co}(\text{NH}_3)_6^{3+}$ ions induced an approximately four-fold stronger inhibitory effect on Pb^{2+} cleavage at C24 than Mg^{2+} ions. This is in agreement with previously published NMR data (49) where about an eight-fold stronger binding of $\text{Co}(\text{NH}_3)_6^{3+}$ than of Mg^{2+} was

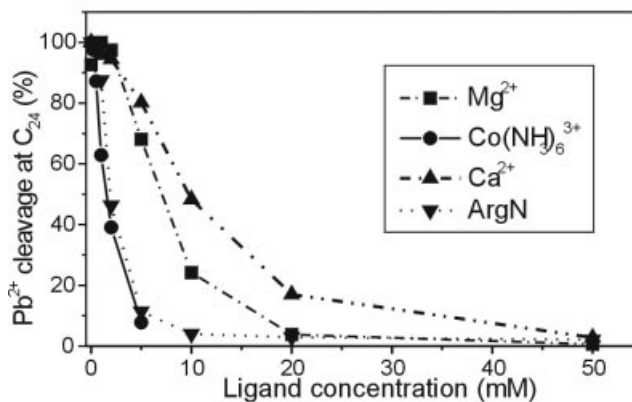
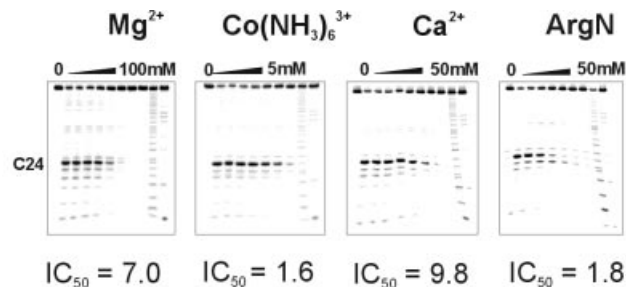


Figure 4. The comparison of inhibitory effects of Mg^{2+} , $\text{Co}(\text{NH}_3)_6^{3+}$, Ca^{2+} and argininamide on 2 mM Pb^{2+} induced cleavage of TAR RNA at C24 position of the bulge. The concentrations of ligands resulting in 50% inhibition (IC_{50}) of the Pb^{2+} -induced cleavage are indicated.

observed within RNA pseudoknot. Interestingly, also argininamide, our reference molecule, inhibits lead-induced cleavage with estimated value of $\text{IC}_{50} = 1.8$ mM (Fig. 4). The obtained value of IC_{50} for this interaction is close to that determined for $\text{Co}(\text{NH}_3)_6^{3+}$. The result of this experiment provides further evidence that the bulge region of free TAR is a specific metal ion-binding site.

Targeting of HIV-1 TAR RNA by magnesium ions using Brownian dynamics simulations

The ligand-free HIV-1 TAR RNA structure derived from NMR study (36) was deposited in a form of 20 relatively spread out conformers (PDB code 1ANR), which reflect the dynamic character of this molecule. Therefore, instead of making any arbitrary selection of one of them, which in our case would certainly limit the value of results obtained, we decided to perform BD simulation on the whole set. In our calculations we did not do any limitation to the data obtained (31) but considered all 1000 steps for each trajectory. The contours (see Materials and Methods) were very well resolved, thus allowing for the localisation of potential magnesium binding sites. The 'number of contacts' was used as a measure of occupancy levels for each site. Because of space limitation, only one selected structure (no. 7) is presented in Figure 5. Table 1 shows the sites of HIV-1 TAR RNA that are most often targeted by magnesium ions within the structures of high and medium occupancy level.

Despite the considerable diversity of all 20 TAR coordinates (average RMSD in the range of 5 Å), BD simulations clearly revealed that for 14 cases, the bulge region was

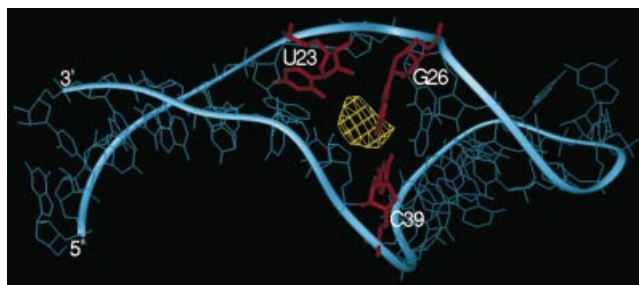


Figure 5. Selected TAR RNA conformer (no. 7 of 1ANR PDB file) targeted by Mg^{2+} as provided by the BD simulations. Yellow contour indicates the postulated magnesium location and the TAR RNA residues closest to it are presented in red.

Table 1. The sites of HIV-1 TAR RNA most often targeted by magnesium ions within the BD simulated structures of high and medium occupancy level

Targeted site	Residues involved	1ANR No.
apical loop	U25(O4), C30(O2), G34(O6)	3
bulge	A20(N6), A20(N7), U23(N3), U40(O4)	4
bulge	C24(OP), U42(OP)	6
apical loop	A27(N7), G34(O6)	
bulge	U23(O2), G26(O6), C39(N4)	7
bulge	U23(O4'), C24(OP), U40(N2)	10
bulge	U23(OP), U23(O5'), C24(OP), G26(N2)	12
bulge	U23(O2'), U40(O4), U40(N3)	16
apical loop	U31(OP), G32(OP), G33(OP), G34(O6)	19

targeted by magnesium ions. In eight out of 14 mentioned cases, one or two magnesium binding sites were localised within the area composed of U23-C24-U25 bulge residues and flanking base pairs A22-U40 and G26-C39. For another six cases, the residues of the bulge and also stems or the apical loop created one or two magnesium binding sites. Interestingly, G34 is most often found as a contacting residue at the apical loop region. Only two conformers with magnesium bound solely in the apical loop region were found. Two structures with three well resolved magnesium sites were predicted by BD simulation. For four strongly bent TAR conformers both stems are 'bridged' by magnesium. This observation closely resembles the result of a BD simulation of neomycin cation binding to TAR RNA where the ligand preferentially spans the lower and upper stem (42).

Are the results of BD simulation related to our experimental data? One might conclude from the BD simulation that it is the region of the bulge which is predominately targeted by magnesium. This would certainly fit and complement the experimental data presented above. At this stage, the protocol of the BD data analysis was oriented towards targeting RNA, i.e. to point at potential magnesium ion binding sites. Therefore, it was not designed to show the conformational consequences of metal ion binding. In the second stage of our studies, which will involve time-restricted molecular

dynamics, the results obtained from BD simulations of TAR RNA/magnesium will serve as starting points to provide highly resolved structures. Only at that level of accuracy, with explicit solvent included, will we be in the position to answer the above question and comment on the different ability of certain TAR RNA conformers (different occupancy levels) to capture metal ions. In fact, dealing with the plethora of TAR RNA structures would be very informative for describing structural factors of RNA-ion binding specificity.

CONCLUSIONS

Relatively weak RNA intermolecular interactions, including RNA/metal ion binding, may play important biological roles. In this study we have shown that Mg^{2+} , Ca^{2+} and $Co(NH_3)_6^{3+}$ bind to the bulge region of HIV-1 TAR RNA. Results obtained from ^{19}F NMR spectroscopy are consistent with those of the metal ion-induced cleavages and competition experiments—the binding of metal ions in solution is weak, in the millimolar range, but specific. The authors of the X-ray structural study on the RNA bulged duplex of native TAR RNA sequence (44) suggested that the presence of four calcium ions in the crystal structure might be indicative of a potential divalent metal ion-binding site within the native TAR RNA. The results of our studies in solution are in agreement with that conclusion and with previous findings concerning both straightening of a TAR RNA bulged duplex (45) and the inhibition of TAR/Tat-peptide binding (46), which were both induced by Mg^{2+} ions. The BD simulation conducted on the set of 20 NMR-derived coordinates indicated that the bulge region of the HIV-1 TAR RNA was predominately targeted by $Mg(H_2O)_6^{2+}$ cations. Combining the approaches of ^{19}F NMR spectroscopy, metal ion-induced RNA cleavages and BD simulations offers a versatile way for the exploration of moderately weak binding of metal ions to RNA in solution.

ACKNOWLEDGEMENTS

The authors thank M. J. Gait for discussion and J. A. McCammon and J. Briggs for kindly supplying us with the UHBD software. This work was supported by the State Committee for Scientific Research, Republic of Poland (grant 6 P04 A04917). The generous support of the Poznań Supercomputing and Networking Centre is acknowledged.

REFERENCES

- Teeter, M.M., Quigley, G.J. and Rich, A. (1980) Metal ions and transfer RNA. In Spiro, T.G. (ed.), *Nucleic Acid-Metal Ion Interactions*. Wiley, New York, pp. 145–177.
- Feig, A.L. and Uhlenbeck, O.C. (1999) The role of metal ions in RNA biochemistry. In Gesteland, R.F., Cech, T. and Atkins, J.F. (eds), *The RNA World*. Cold Spring Harbor Laboratory Press, Cold Spring Harbor, NY, pp. 287–319.
- Cate, J.H., Gooding, A.R., Podell, E., Zhou, K.H., Golden, B.L., Kundrot, C.E., Cech, T.R. and Doudna, J.A. (1996) Crystal structure of a group I ribozyme domain: principles of RNA packing. *Science*, **273**, 1678–1685.
- Misra, V.K. and Draper, D.E. (1998) On the role of magnesium ions in RNA stability. *Biopolymers*, **48**, 113–135.
- Misra, V.K. and Draper, D.E. (2001) A thermodynamic framework for Mg^{2+} binding to RNA. *Proc. Natl Acad. Sci. USA*, **98**, 12456–12461.

6. Jack, A., Ladner, J.E., Rhodes, D., Brown, R.S. and Klug, A. (1977) A crystallographic study of metal-binding to yeast phenylalanine transfer RNA. *J. Mol. Biol.*, **111**, 315–328.
7. Jovine, L., Djordjevic, S. and Rhodes, D. (2000) The crystal structure of yeast phenylalanine tRNA at 2.0 Å resolution: cleavage by Mg(2+) in 15-year old crystals. *J. Mol. Biol.*, **301**, 401–414.
8. Scott, W.G., Murray, J.B., Arnold, J.R., Stoddard, B.L. and Klug, A. (1996) Capturing the structure of a catalytic RNA intermediate: the hammerhead ribozyme. *Science*, **274**, 2065–2069.
9. Cate, J.H., Hanna, R.L. and Doudna, J.A. (1997) A magnesium ion core at the heart of a ribozyme domain. *Nature Struct. Biol.*, **4**, 553–558.
10. Wedekind, J.E. and McKay, D.B. (1999) Crystal structure of a lead-dependent ribozyme revealing metal binding sites relevant to catalysis. *Nature Struct. Biol.*, **6**, 261–268.
11. Correll, C.C., Freeborn, B., Moore, P.B. and Steitz, T.A. (1997) Metals, motifs, and recognition in the crystal structure of a 5S rRNA domain. *Cell*, **91**, 705–712.
12. Kieft, J.S. and Tinoco, I. (1997) Solution structure of a metal-binding site in the major groove of RNA complexed with cobalt (III) hexamine. *Structure*, **5**, 713–721.
13. Gonzalez, R.L. and Tinoco, I. (2001) Identification and characterization of metal ion binding sites in RNA. *Methods Enzymol.*, **338**, 421–443.
14. Hardin, C.C., Gollnick, P., Kallenbach, N.R., Cohn, M. and Horowitz, J. (1986) Fluorine-19 nuclear magnetic resonance studies of the structure of 5-fluorouracil-substituted *Escherichia coli* transfer RNA. *Biochemistry*, **25**, 5699–5709.
15. Chu, W.C., Kintanar, A. and Horowitz, J. (1992) Correlations between fluorine-19 nuclear magnetic resonance chemical shift and the secondary and tertiary structure of 5-fluorouracil-substituted tRNA. *J. Mol. Biol.*, **227**, 1173–1181.
16. Sahasrabudhe, P.V., Pon, R.T. and Gmeiner, W.H. (1995) Effects of site-specific substitution of 5-fluorouridine on the stabilities of duplex DNA and RNA. *Nucleic Acids Res.*, **23**, 3916–3921.
17. Fischer, A., Gdaniec, Z., Biala, E., Lozynski, M., Milecki, J. and Adamiak, R.W. (1996) F-19 NMR of RNA. The structural and chemical aspects of 5-fluoro-cytidine and -uridine labelling of oligoribonucleotides. *Nucl. Nucl.*, **15**, 477–488.
18. Kanyo, J.E., Duhamel, J. and Lu, P.Z. (1996) Secondary structure of the r(CUUCGG) tetraloop. *Nucleic Acids Res.*, **24**, 4015–4022.
19. Arnold, J.R.P. and Fisher, J. (2000) Structural equilibria in RNA as revealed by F-19 NMR. *J. Biomol. Struct. Dyn.*, **17**, 843–856.
20. Hammann, C., Norman, D.G. and Lilley, D.M.J. (2001) Dissection of the ion-induced folding of the hammerhead ribozyme using F-19 NMR. *Proc. Natl Acad. Sci. USA*, **98**, 5503–5508.
21. Ciesiolka, J., Wrzesinski, J., Gornicki, P., Podkowinski, J. and Krzyzosiak, W.J. (1989) Analysis of magnesium, europium and lead binding sites in methionine initiator and elongator tRNAs by specific metal-ion-induced cleavages. *Eur. J. Biochem.*, **186**, 71–77.
22. Polacek, N. and Barta, A. (1998) Metal ion probing of rRNAs: evidence for evolutionarily conserved divalent cation binding pockets. *RNA*, **4**, 1282–1294.
23. Matysiak, M., Wrzesinski, J. and Ciesiolka, J. (1999) Sequential folding of the genomic ribozyme of the hepatitis delta virus: structural analysis of RNA transcription intermediates. *J. Mol. Biol.*, **291**, 283–294.
24. Kazakov, S. and Altman, S. (1991) Site-specific cleavage by metal ion cofactors and inhibitors of M1 RNA, the catalytic subunit of RNase P from *Escherichia coli*. *Proc. Natl Acad. Sci. USA*, **88**, 9193–9197.
25. Streicher, B., von Ahsen, U. and Schroeder, R. (1993) Lead cleavage sites in the core structure of group I intron-RNA. *Nucleic Acids Res.*, **21**, 311–317.
26. Ciesiolka, J. (1999) Metal ion-induced cleavages in probing of RNA structure. In Barciszewski, J. and Clarke, B.F.C. (eds), *RNA Biochemistry and Biotechnology*. Kluwer Academic Publishers, Dordrecht, The Netherlands, pp. 111–121.
27. Streicher, B., Westhof, E. and Schroeder, R. (1996) The environment of two metal ions surrounding the splice site of a group I intron. *EMBO J.*, **15**, 2556–2564.
28. Winter, D., Polacek, N., Halama, I., Streicher, B. and Barta, A. (1997) Lead-catalysed specific cleavage of ribosomal RNAs. *Nucleic Acids Res.*, **25**, 1817–1824.
29. Fischer, A., Gdaniec, Z., Olejniczak, M., Bielecki, L. and Adamiak, R.W. (1999) Does 29-mer RNA hairpin of the HIV-1 TAR RNA sequence bind magnesium? ¹⁹F-NMR and modelling studies. *Nucleic Acids Symp. Ser.*, **42**, 117–118.
30. Gdaniec, Z., Sierzputowska-Gracz, H. and Theil, E.C. (1998) Iron regulatory element and internal loop/bulge structure for ferritin mRNA studied by cobalt(III) hexamine binding, molecular modeling, and NMR spectroscopy. *Biochemistry*, **37**, 1505–1512.
31. Hermann, T. and Westhof, E. (1998) Exploration of metal ion binding sites in RNA folds by Brownian-dynamics simulations. *Struct. Fold. Des.*, **6**, 1303–1314.
32. Jossinet, F., Paillart, J.C., Westhof, E., Hermann, T., Skripkin, E., Lodmell, J.S., Ehresmann, C., Ehresmann, B. and Marquet, R. (1999) Dimerization of HIV-1 genomic RNA of subtypes A and B: RNA loop structure and magnesium binding. *RNA*, **5**, 1222–1234.
33. van Buuren, B.N.M., Hermann, T., Wijmenga, S.S. and Westhof, E. (2002) Brownian-dynamics simulations of metal-ion binding to four-way junctions. *Nucleic Acids Res.*, **30**, 507–514.
34. Jones, K.A. and Peterlin, B.M. (1994) Control of RNA initiation and elongation at the HIV-1 promoter. *Annu. Rev. Biochem.*, **63**, 717–743.
35. Hamy, F., Felder, E.R., Heizmann, G., Lazdins, J., Aboul-ela, F., Varani, G., Karn, J. and Klimkait, T. (1997) An inhibitor of the Tat/TAR RNA interaction that effectively suppresses HIV-1 replication. *Proc. Natl Acad. Sci. USA*, **94**, 3548–3553.
36. Aboul-ela, F., Karn, J. and Varani, G. (1996) Structure of HIV-1 TAR RNA in the absence of ligands reveals a novel conformation of the trinucleotide bulge. *Nucleic Acids Res.*, **24**, 3974–3981.
37. Aboul-ela, F., Karn, J. and Varani, G. (1995) The structure of the human immunodeficiency virus type-1 TAR RNA reveals principles of RNA recognition by Tat protein. *J. Mol. Biol.*, **253**, 313–332.
38. Nifosi, R., Reyes, C.M. and Kollman, P.A. (2000) Molecular dynamics studies of the HIV-1 TAR and its complex with argininamide. *Nucleic Acids Res.*, **28**, 4944–4955.
39. Puglisi, J.D., Tan, R., Calnan, B.J., Frankel, A.D. and Williamson, J.R. (1992) Conformation of the TAR RNA-arginine complex by NMR spectroscopy. *Science*, **257**, 76–80.
40. Long, K.S. and Crothers, D.M. (1999) Characterization of the solution conformations of unbound and Tat peptide-bound forms of HIV-1 TAR RNA. *Biochemistry*, **38**, 10059–10069.
41. Faber, C., Sticht, H., Schweimer, K. and Rosch, P. (2000) Structural rearrangements of HIV-1 Tat-responsive RNA upon binding of neomycin B. *J. Biol. Chem.*, **275**, 20660–20666.
42. Hermann, T. and Westhof, E. (1999) Docking of cationic antibiotics to negatively charged pockets in RNA folds. *J. Med. Chem.*, **42**, 1250–1261.
43. Al-Hashimi, H.M., Gosser, Y., Gorin, A., Majumdar, W.H.A. and Patel, D.J. (2002) Concerted motions in HIV-1 TAR RNA may allow access to bound state conformations: RNA dynamics from NMR residual dipolar couplings. *J. Mol. Biol.*, **315**, 95–102.
44. Ippolito, J.A. and Steitz, T.A. (1998) A 1.3-angstrom resolution crystal structure of the HIV-1 trans-activation response region RNA stem reveals a metal ion-dependent bulge conformation. *Proc. Natl Acad. Sci. USA*, **95**, 9819–9824.
45. Zacharias, M. and Hagerman, P.J. (1995) The bend in RNA created by the trans-activation response element bulge of human immunodeficiency virus is straightened by arginine and by Tat-derived peptide. *Proc. Natl Acad. Sci. USA*, **92**, 6052–6056.
46. Arzumanov, A., Godde, F., Moreau, S., Toulme, J.J., Weeds, A. and Gait, M.J. (2000) Use of the fluorescent nucleoside analogue benzo[g]quinazoline 2'-O-methyl-beta-D-ribofuranoside to monitor the binding of the HIV-1 Tat protein or of antisense oligonucleotides to the TAR RNA stem-loop. *Helv. Chim. Acta*, **83**, 1424–1436.
47. Usman, N., Ogilvie, K.K., Jiang, M.-Y. and Cedergren, R.J. (1987) Automated chemical synthesis of long oligoribonucleotides using 2'-O-silylated ribonucleoside 3'-O-phosphoramidites on a controlled-pore glass support: synthesis of a 43-nucleotide sequence similar to the 3' half of an *Escherichia coli* formylmethionine tRNA. *J. Am. Chem. Soc.*, **109**, 7845–7854.
48. Fielding, L. (2000) Determination of association constants (K_a) from solution NMR data. *Tetrahedron*, **56**, 6151–6170.
49. Gonzalez, R.L. and Tinoco, I. (1999) Solution structure and thermodynamics of a divalent metal ion binding site in an RNA pseudoknot. *J. Mol. Biol.*, **289**, 1267–1282.
50. Madura, J.D., Davis, M.E., Gilson, M.K., Wade, R.C., Luty, B.A. and McCammon, J.A. (1994) Biological applications of electrostatic calculations and Brownian-dynamics simulations. *Rev. Comp. Chem.*, **5**, 229–267.

51. Sahasrabudhe,P.V. and Gmeiner,W.H. (1997) Solution structures of 5-fluorouracil-substituted RNA duplexes containing G-U wobble base pairs. *Biochemistry*, **36**, 5981–5991.
52. Colmenarejo,G. and Tinoco,I. (1999) Structure and thermodynamics of metal binding in the P5 helix of a group I intron ribozyme. *J. Mol. Biol.*, **290**, 119–135.
53. Traut,T.W. (1994) Physiological concentrations of purines and pyrimidines. *Mol. Cell. Biochem.*, **140**, 1–22.
54. Cowan,J.A. (1993) Metallobiochemistry of RNA. Co(NH₃)₆(3+) as a probe for Mg²⁺(aq) binding sites. *J. Inorg. Biochem.*, **49**, 171–175.
55. Butcher,S.E., Allain,F.H.T. and Feigon,J. (2000) Determination of metal ion binding sites within the hairpin ribozyme domains by NMR. *Biochemistry*, **39**, 2174–2182.
56. Rudisser,S. and Tinoco,I. (2000) Solution structure of cobalt(III)hexammine complexed to the GAAA tetraloop, and metal-ion binding to G·A mismatches. *J. Mol. Biol.*, **295**, 1211–1223.
57. Kierzek,R. (2001) Nonenzymatic cleavage of oligoribonucleotides. *Methods Enzymol.*, **341**, 657–675.
58. Kaukinen,U., Lyytikainen,S., Mikkola,S. and Lonnberg,H. (2002) The reactivity of phosphodiester bonds within linear single-stranded oligoribonucleotides is strongly dependent on the base sequence. *Nucleic Acids Res.*, **30**, 468–474.